

# Kinetics and Mechanism of Hydrothermal Decomposition of Lignin Model Compounds

Xiaoyu Wu,<sup>†,‡</sup> Jie Fu,<sup>\*,†</sup> and Xiuyang Lu<sup>\*,†</sup>

<sup>†</sup>Key Laboratory of Biomass Chemical Engineering of Ministry of Education, Department of Chemical and Biological Engineering, Zhejiang University, Hangzhou 310027, China

<sup>‡</sup>School of Chemical Engineering & Pharmacy, Wuhan Institute of Technology, Wuhan, 430073, Hubei, China

**S** Supporting Information

**ABSTRACT:** The kinetics and underlying mechanisms of the hydrothermal decomposition of the lignin model compounds anisole, diphenyl ether and phenethyl phenyl ether were studied. Whereas diphenyl ether was stable at hydrothermal conditions, anisole and phenethyl phenyl ether underwent hydrothermal decomposition between 260 and 290 °C. Experiments involving different initial reactant concentrations and different batch holding times revealed that hydrolysis of both anisole and phenethyl phenyl ether followed first-order kinetics. Experiments at different temperatures showed that the first-order rate constants displayed Arrhenius behavior, with activation energies of  $149.8 \pm 16.4$  and  $143.2 \pm 21.0$  kJ·mol<sup>-1</sup> for anisole and phenethyl phenyl ether, respectively. A reaction mechanism is proposed for anisole, and reaction pathways for the decomposition of phenethyl phenyl ether are proposed based on the distribution of the products generated by hydrolysis. The reactivity of ether hydrothermal decomposition is discussed by reviewing the published conversion data of other ethers.

## 1. INTRODUCTION

Diminishing petroleum reserves and growing concerns about global climate change necessitate the development of fuel and chemical production pathways based on biomass resources. Biomass mainly consists of cellulose, lignin, and hemicellulose, with lignin contributing approximately 15–30% of the total mass.<sup>1</sup> As a biopolymer in which hydroxyphenylpropane units such as *trans-p*-coumaryl alcohol, coniferyl alcohol, and sinapyl alcohol are connected with ether and carbon–carbon bonds,<sup>2</sup> lignin thus represents a promising, yet underexploited, potential source of phenolic chemicals. Accordingly, studies devoted to obtaining high value chemicals, such as phenol, *o*-cresol, and catechol, as well as other intermediates derived from the decomposition of lignin, have thus attracted much attention.

High-temperature water, defined as liquid water above 180 °C, is a green medium for chemical reactions. High-temperature water exhibits properties that are very different from those of liquid water at ambient temperatures. It has a lower dielectric constant, fewer and weaker hydrogen bonds, and a higher ion product than the water at room temperature ( $K_w$ ). These properties of high-temperature water vary with temperature and pressure (or density) over wide ranges at near-critical and supercritical conditions. The high natural concentrations of the H<sup>+</sup> and OH<sup>-</sup> ions resulting from the high  $K_w$  of high-temperature water facilitate both acid- and base-catalyzed reactions.<sup>3,4</sup>

More than two-thirds of the bonds in the structure of lignin are ether bonds,<sup>5</sup> hydrolytic cleavage of which can be catalyzed by either [H<sup>+</sup>] and [OH<sup>-</sup>], or water molecules.<sup>6</sup> Wahyudiono et al.<sup>1</sup> and Yokoyama et al.<sup>7</sup> demonstrated that lignin could be mainly decomposed by hydrolysis of ether bonds in near-critical water and that C–C bonds were also broken under supercritical conditions. The increase in temperature could promote the reaggregation of small aromatic molecules derived from lignin.

Analysis of hydrothermal degradation products of biomass, such as switchgrass<sup>8</sup> and rice bran,<sup>9</sup> identified several aromatic chemicals, including protocatechuic acid, *p*-hydroxybenzoic acid, and vanillic acid. However, the hydrothermal decomposition of lignin or wood biomass involves many reactions, and the reaction pathways and mechanism of lignin decomposition have not been well demonstrated. A better understanding of these reactions will be essential to improve the efficiency with which lignin is used.

Ether linkages in the structure of lignin can be any of the methoxy linkage, 4-O-5 linkage,  $\alpha$ -O-4 linkage, and  $\beta$ -O-4 linkage types. Recently, our group used benzyl phenyl ether (BPE) as the model compound for the  $\alpha$ -O-4 linkage and successfully converted BPE to phenol (>76% selectivity) and benzyl alcohol (>83% selectivity) under hydrothermal conditions.<sup>10</sup> However, there appears to have been no systematic analysis of the hydrothermal reactivity of other ether linkages.

In this study, anisole (**1**), diphenyl ether (**2**), and phenethyl phenyl ether (PPE, **3**) were selected as model compounds to study the methoxy linkage, 4-O-5 linkage, and  $\beta$ -O-4 linkage, respectively. Figure 1 shows the structures of these three compounds. Our analysis of the product distributions and kinetics for hydrothermal decomposition of these model compounds is the first to systematically study the hydrothermal reaction behaviors of ether linkages of lignin. The results also provide insights into the relationship between ether structure and hydrothermal reactivity.

**Received:** October 22, 2012

**Revised:** March 7, 2013

**Accepted:** March 17, 2013

**Published:** March 17, 2013

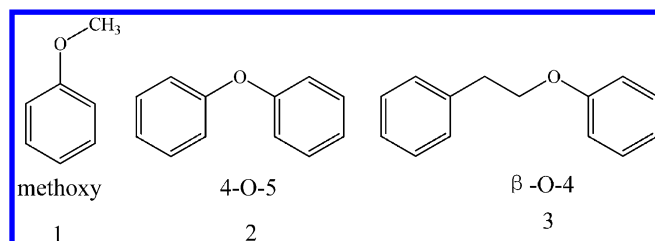


**Figure 1.** Structure of lignin model compounds in this study: (1) anisole, (2) diphenyl ether, (3) phenethyl phenyl ether.

## 2. MATERIALS AND METHODS

**2.1. Materials.** Anisole ( $\geq 98.0\%$ ), diphenyl ether ( $\geq 99.0\%$ ), phenol ( $\geq 99.5\%$ ), methanol ( $\geq 99.5\%$ ), acetic acid ( $\geq 99.5\%$ ), *n*-octanol ( $\geq 99.5\%$ ), and sodium hydroxide ( $\geq 96.0\%$ ) were purchased from Sinopharm Chemical Reagent Co. Ltd., China; (2-bromoethyl) benzene ( $\geq 99\%$ ) was obtained from J&K Chemical Industry Co. LTD, China. These chemicals are all analytical reagent grade. We prepared PPE (98% purity) by reacting (2-bromoethyl) benzene with phenol, as described previously.<sup>11</sup> Deionized water was prepared in-house.

**2.2. Reactor.** The batch reactor, made of 316L stainless steel tubing, had a volume of approximately 13.5 mL. It was constructed from three parts: a tube, a stopper, and a cap. The internal diameter of the tube was 12 mm. It was sealed by a stopper, which had a seal diameter of 13.8 mm. A cap was employed to tighten the tube and stopper. The reactor can function under pressures of up to 20 MPa and temperatures of up to 290 °C. It was heated by a steel box furnace that could heat up to 12 reactors simultaneously. The furnace could maintain the temperature within  $\pm 2\%$  of the designated temperature.

**2.3. Experimental Procedure.** A carefully measured amount of the reactant of interest was added to the reaction vessel, which was then loaded with 10 mL of water and quickly heated by immersing it in a steel box furnace preheated to an adequate temperature. Thus, these experiments took place essentially under the water saturation vapor pressure at each reaction temperature. After the desired time had elapsed, excluding the heating time of approximately 20 min, the reactor was moved to a water bath to quench the reaction. The reactor contents were transferred to a 25 mL volumetric flask (for anisole) or a 50 mL volumetric flask (for diphenyl ether and phenethyl phenyl ether), and the reactors were subsequently rinsed with repeated methanol washes until the total volume had been collected. Standard deviations were determined from three replicate experiments.

**2.4. Analysis.** For different lignin model compounds, two quantitative analysis methods were established. The samples from the experiments of anisole were analyzed using an Agilent model 1790 gas chromatograph equipped with a flame ionization detector. *n*-Octanol was added to the samples as an internal standard. A 30 m  $\times$  0.32 mm  $\times$  0.25  $\mu$ m DB1701 capillary column with nitrogen carrier gas was used to separate the sample components. The temperature of both the injector and detector was 160 °C, and the temperature of the oven was maintained at 80 °C. The injection volume was 0.2  $\mu$ L.

The samples from the experiments involving diphenyl ether and PPE were analyzed using the external reference method with an Agilent 1100 high-pressure liquid chromatograph (HPLC1100) equipped with a UV detector. A 4 mm i.d.  $\times$  250

mm KNAUER C18 reverse-phase column was used, and the column temperature was maintained at 35 °C. The flow rate of the mobile phase was 0.5 mL/min, with gradient elution involving different relative volumes of 0.2% acetic acid solution and methanol (0–20 min, 80:20–60:40; 20–40 min, 60:40–20:80; 40–45 min, 20:80–10:90; 45–55 min, 10:90–80:20, post time 10 min). The injection volume was 5  $\mu$ L. Analysis of standard solution with known amounts of the compounds of interest provided calibration curves, which were used to determine the amount of each component in the reaction samples.

Products were identified by comparison of retention times with those of standard solutions of pure compounds, and the identities were confirmed using GC-MS (Agilent 6890GC/5973 MSD).

## 3. RESULTS AND DISCUSSION

This section provides the experimental results for the hydrothermal decomposition of three lignin model compounds at different initial concentrations of reactant, different heating times, and different temperatures. Moreover, related reaction mechanisms and pathways are proposed, and the reactivity of ether hydrothermal decomposition is discussed.

**3.1. Hydrothermal Decomposition of Anisole.** Figure 2 shows the effect of the initial concentration of anisole on its

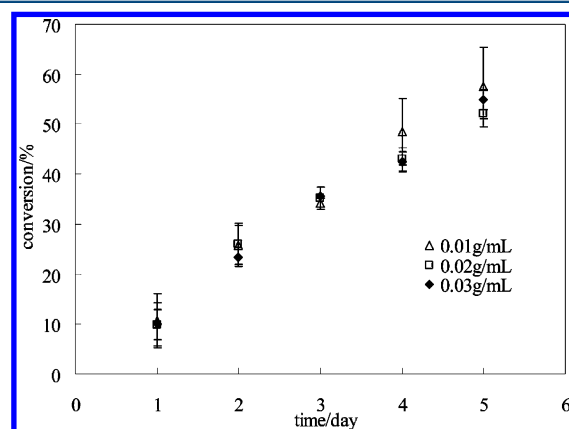


**Figure 2.** Temporal variation of anisole conversion at different initial concentrations.

hydrothermal decomposition at 280 °C. The standard deviations in Figure 2 were determined from three replicate experiments. The conversion of anisole was about 60% for 5 days at 280 °C. The conversion rates of anisole were similar at 0.01, 0.02, and 0.03 g/mL. The conversions were invariant under different concentrations, signaling first-order kinetics for the hydrothermal decomposition.

Figure 3a shows the effect of temperature on the anisole conversion. The experiments were performed at 260, 270, 280, and 290 °C, with an initial anisole concentration of 0.02 g/mL. The standard deviations in Figure 3a were determined from three replicate experiments. The conversion of anisole was affected by both temperature and time. The conversion of anisole was 74.2% at 290 °C after 4 days. At 260 °C, on the other hand, the conversion was only 12.1% after 4 days. At the same temperature (290 °C), the conversion of anisole was 74.2% after 4 days, which is much higher than that after 1 day (29.5%). The curves in Figure 3 were calculated from a first-order rate equation, as will be described later in this paper.

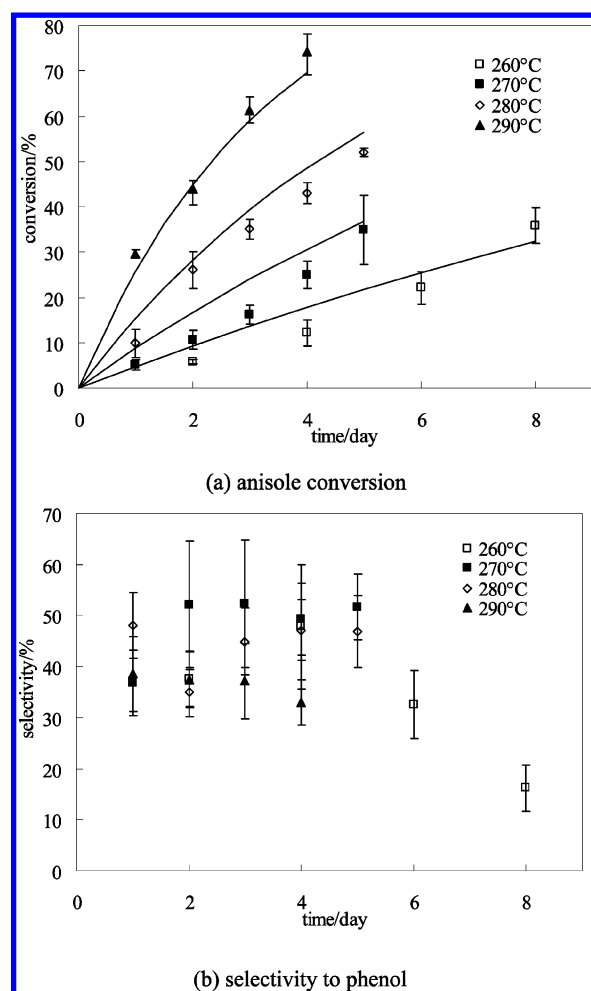


Figure 3. Temporal variation of anisole conversion and selectivity to phenol at different temperatures.

Phenol was the only product detected by GC-MS. The GC-MS spectrum is presented in the Supporting Information. Figure 3b shows the selectivity to phenol from the decomposition at 260, 270, 280, and 290 °C. The standard deviations in Figure 3b were determined from three replicate experiments. The large error bars are likely due to difficulties in recovering all of the material from the reaction systems. The maximum selectivity was only 52.3% at 270 °C after 3 days. In the temperature range of 270–290 °C, the selectivity decreased as the reaction temperature increased, and the selectivity decreased as reaction time elapsed at all temperatures. At 280 °C, the selectivity was 44.9% after 3 days, which is higher than that at 290 °C after 3 days (37.2%). At 290 °C, the selectivity after 1 day (38.5%) was higher than that after 4 days (32.9%), and similar trend was found at 260 °C. This indicates that higher temperature and longer reaction times promoted the conversion of phenol to other products, via reactions such as the condensation of phenol from thermodynamically favored phenoxyl.<sup>10</sup>

The decomposition of ethers in neutral water was attributed to the protons generated by the self-dissociation of water and coexisting H<sub>2</sub>O catalyst.<sup>6</sup> Protons or water interacted with ether oxygen to form an intermediate (ether–H<sup>+</sup>), which can be decomposed through either of S<sub>N</sub>1 or S<sub>N</sub>2 mechanisms. In general, the S<sub>N</sub>1 mechanism predominates during decomposition of aryl–aryl ethers to form stable carbocations. In

contrast, the S<sub>N</sub>2 mechanism involves formation of an ion pair from OH<sup>−</sup> or H<sub>2</sub>O and ether–H<sup>+</sup> in a transition state, as occurs during the decomposition of alkyl–aryl ethers.<sup>12</sup> For anisole, the Ph–O bond is difficult to break, because the electronic conjugation between the benzene ring and oxygen increases the electron density and bond strength of the Ph–O bond. In addition, like other alkyls, the methyl group cannot form a stable carbocation. Therefore, anisole, as an alkyl–aryl ether, is probably degraded via S<sub>N</sub>2 mechanisms. The proposed reaction mechanism for the decomposition of anisole is shown in Figure 4. Anisole is decomposed via the S<sub>N</sub>2 mechanism to yield a

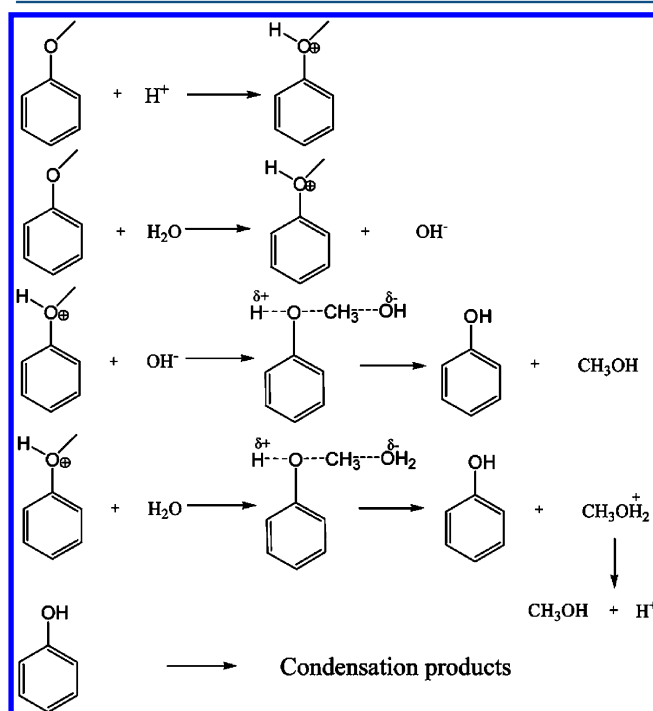


Figure 4. Proposed reaction mechanism for decomposition of anisole.

phenol and a methanol carbocation, which was subsequently degraded into methanol and a proton. The proton can then participate in the formation of the ether–H<sup>+</sup> intermediate.

### 3.2. Hydrothermal Decomposition of Diphenyl Ether.

No conversion was observed when a diphenyl ether solution (0.02 g/mL) was placed in the reactor at 290 °C for 5 days. The failure to detect a product using HPLC analysis indicates that diphenyl ether was stable under hydrothermal conditions.

### 3.3. Hydrothermal Decomposition of Phenethyl Phenyl Ether (PPE).

Figure 5 shows the effect of the initial concentration of PPE on its hydrothermal decomposition at 280 °C. The standard deviations in Figure 5 were determined from three replicate experiments. The conversion rates of PPE were similar at all concentrations, which indicates that first-order kinetics govern the hydrothermal decomposition. Compared to anisole, PPE was more reactive under hydrothermal conditions, and its conversion was 39.3% complete after heating to 280 °C for 25 h.

Figure 6a shows the effect of temperature on the PPE conversion. The experiments were conducted at 260, 270, 280, and 290 °C, with an initial PPE concentration of 0.02 g/mL. The standard deviations in Figure 6a were determined from three replicate experiments. Both the reaction temperature and time influenced the conversion of PPE. At 260 °C, the

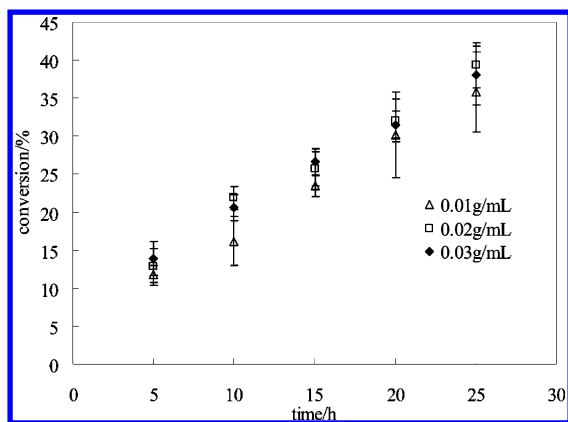


Figure 5. Temporal variation of PPE conversion at different initial concentrations.

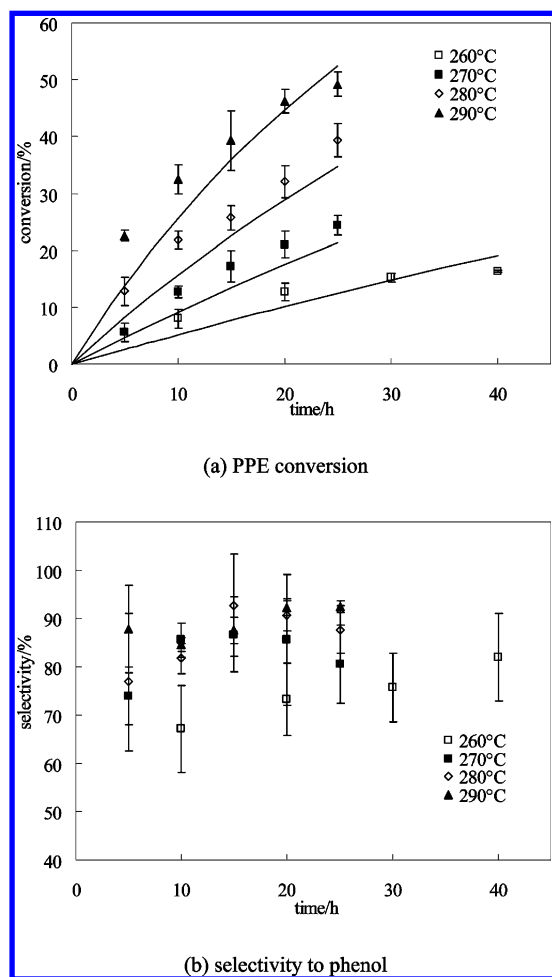


Figure 6. Temporal variation of PPE conversion and selectivity to phenol at different temperatures.

conversion of PPE was 12.8% after 20 h, which is much lower than that at 290 °C after 20 h (46.3%). At the same temperature (290 °C), the conversion of PPE was 49.2% after 25 h, which is much higher than that after 5 h (22.5%). The smooth curves were again from a first-order kinetics model that will be discussed in the next section.

Figure 6b shows the effect of temperature on phenol selectivity. The standard deviations in Figure 6b were determined from three replicate experiments. There were no

significant differences in the selectivity at 270, 280, and 290 °C at each reaction time, and most of them were approximately 80–92%. Again, the selectivities at 260 °C were lower than those at other temperatures. This phenomenon was inconsistent with the decrease in selectivity of BPE decomposition for phenol as the temperature increased.<sup>10</sup>

As shown in Figure 7, analysis of the PPE sample using GC-MS identified other products as  $\beta$ -phenylethyl alcohol (3),  $\alpha$ -phenylethyl alcohol (7), styrene (5), phenylacetaldehyde (6), acetophenone (8), ethylbenzene (9), benzaldehyde (10), benzoic acid (11), and 2-(1-phenylethyl)phenol (4). The GC-MS spectrum is presented in the Supporting Information.  $\beta$ -Phenylethyl alcohol (3) was the product of PPE hydrolysis. Styrene (5) could be the primary product from the thermal decomposition of PPE<sup>11,13</sup> and could also be generated by the reversible dehydration of  $\beta$ -phenylethyl alcohol (3), which was demonstrated by the identification of styrene (5) through GC-MS analysis of the sample following reaction with  $\beta$ -phenylethyl alcohol (3) at 280 °C for 20 h. However, owing to its strong reactivity, styrene (5) was prone to oligomerization, resulting in low yield.  $\alpha$ -Phenylethyl alcohol (7) was also identified by GC-MS in the sample, using  $\beta$ -phenylethyl alcohol as a reactant (3). Therefore, the reaction of  $\alpha$ -phenylethyl alcohol (7) was proposed: PPE was first degraded into  $\beta$ -phenylethyl alcohol, and then further dehydrated to styrene, which was subsequently hydrated to form a small amount of  $\alpha$ -phenylethyl alcohol. Ethylbenzene (9) could also be a product generated by thermal decomposition of PPE and was then converted to acetophenone (8) by oxidation.<sup>13,15</sup> Phenylacetaldehyde (6) and acetophenone (8) were likely formed by  $\beta$ -scission of the oxy radical from dehydrogenation of  $\beta$ -phenylethyl alcohol and  $\alpha$ -phenylethyl alcohol, respectively.<sup>14</sup> Small amounts of benzaldehyde (10) might be yielded via two potential reaction pathways. Whereas one involves thermolysis of PPE,<sup>13,15</sup> the other involved oxidation, as for benzoic acid (11).

The thermodynamic stability of radicals, which provides a quantitative basis for rational design of radical reactions in organic synthesis, can be predicted by their radical stabilization energy (RSE). The more negative the RSE of a radical, the more stable it is.<sup>16</sup> The RSE values of the phenylethyl radical, benzene radical, and ethyl radical were  $-9.2$ ,  $+10.3$ , and  $-13.8$   $\text{kJ}\cdot\text{mol}^{-1}$ , respectively. This indicates that the phenylethyl radical is more stable than the benzene radical and less stable than the ethyl radical. Therefore, with the order of radical stability above, the stability of corresponding carbocation could also be obtained, which was used to determine the mechanism of ether decomposition. The ethyl group is a primary alkyl, and the instability of its carbocation results in aryl-ethyl decomposition via the  $\text{S}_{\text{N}}2$  mechanism. Therefore, it is reasonable to assume that hydrothermal decomposition of PPE is by  $\text{S}_{\text{N}}2$ -mediated cleavage.

**3.4. Reactivity of Ether Linkages of Lignin.** The data describing conversion rates were fitted at each temperature with a first-order rate equation. The values of rate constants ( $\times 10^{-3}$   $\text{h}^{-1}$ ) for the hydrothermal decomposition of anisole were  $2.25 \pm 0.334$ ,  $3.47 \pm 0.362$ ,  $6.17 \pm 0.213$ , and  $13.8 \pm 0.726$  at 260, 270, 280, and 290 °C, respectively. The rate constants ( $\times 10^{-3}$   $\text{h}^{-1}$ ) for the hydrothermal decomposition of PPE were  $4.62 \pm 0.693$ ,  $11.34 \pm 0.576$ ,  $18.83 \pm 1.178$ , and  $26.25 \pm 2.954$  at 260, 270, 280, and 290 °C, respectively. The curves in Figures 2a and 5a show that the conversions calculated by the models provided a good representation of the experimental data for

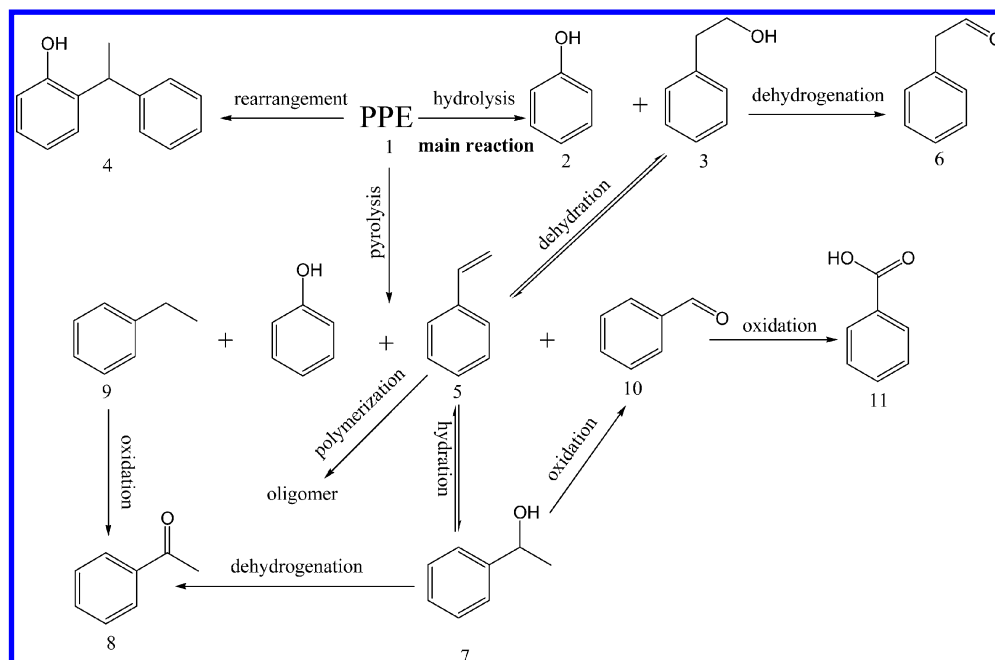


Figure 7. Proposed reaction pathway for decomposition of PPE.

both anisole and PPE at all temperatures. The Arrhenius parameters were determined by linear regression of  $-\ln k$  vs  $1000/RT$  (Table 1).

Table 1. Comparison of Hydrothermal Decomposition Kinetics Parameters for Ether Linkages of Lignin

model compounds	ether linkage	$E_a$ (kJ·mol <sup>-1</sup> )	ln A (h <sup>-1</sup> )	$k$ (h <sup>-1</sup> ) at 260 °C
anisole	methoxy	149.8	27.6	$2.3 \times 10^{-3}$
diphenyl ether	4-O-5			
benzyl phenyl ether <sup>10</sup>	$\alpha$ -O-4	150.3	34.6	2.1
phenethyl phenyl ether	$\beta$ -O-4	143.2	27.1	$4.6 \times 10^{-3}$

Ether linkages are important linkages of lignin, represented by the methoxy linkage, 4-O-5 linkage,  $\alpha$ -O-4 linkage, and  $\beta$ -O-4 linkage. Table 1 summarizes kinetic parameters of the hydrothermal decomposition of the lignin model compounds containing different ether linkages. Whereas the activation energies of the hydrothermal decomposition of the ether model compounds we studied were very similar (except diphenyl ether), the very different reaction rate constants of the four model compounds at 260 °C indicated very different reactivities. Under hydrothermal conditions, the model compound for 4-O-5 linkage (diphenyl ether) was stable. For the methoxy linkage model compound (anisole), the characteristic functional group of lignin, the ether bond could be broken with the rate constant of  $2.3 \times 10^{-3}$  h<sup>-1</sup>. The dominant interunit linkage, which accounts for up to half of the total number of linkages, is the  $\beta$ -O-4 linkage.<sup>13</sup> The rate constant of PPE ( $4.6 \times 10^{-3}$  h<sup>-1</sup>), the simplest model compound for the  $\beta$ -O-4 linkage, was about 2 orders of magnitude larger than for that of the methoxy linkage. However, the rate constant of BPE, the  $\alpha$ -O-4 model compound, was 2.1 h<sup>-1</sup>, which is 450 orders of magnitude larger than that of the  $\beta$ -O-4 model compound (PPE). This might be related to their different reaction mechanisms: whereas hydrolysis of the  $\alpha$ -O-4 model

compound (BPE) could occur via the S<sub>N</sub>1 mechanism involving a stable benzyl carbocation,<sup>10</sup> cleavage of the  $\beta$ -O-4 model compound (PPE) occurred via the S<sub>N</sub>2 mechanism. Interestingly, Minami et al.<sup>17</sup> reported the opposite results for the decomposition of  $\alpha$ -O-4 and  $\beta$ -O-4 linkages in supercritical methanol, with the rate constant of the  $\beta$ -O-4 linkage larger than that of  $\alpha$ -O-4 linkage. This indicates that the reaction solvent plays an important role in the decomposition of the lignin ether bond. Under hydrothermal conditions, cleavage of the lignin ether bond occurred preferentially at the  $\alpha$ -O-4 linkage, and then at the  $\beta$ -O-4 linkage and methoxy linkage, whereas the 4-O-5 linkage was stable.

**3.5. Reactivity of Different Ether Compounds under Hydrothermal Conditions.** We collected the reported conversion data for the hydrothermal decomposition of other ethers at 250 or 230 °C reported in literature<sup>10,18–22</sup> and divided the conversions by the reaction time to obtain the relative conversion rates for each ether, as shown in Table 2. Hydrothermal decomposition of ether was an acid-catalyzed process, and the charged intermediate formed from protonation of the ether by H<sup>+</sup>. The decomposition of the charged intermediate was the rate-determining step.<sup>23</sup> If the charged intermediate was decomposed via S<sub>N</sub>1 mechanism, its conversion rate was faster than that via the S<sub>N</sub>2 mechanism. For example, benzyl phenyl ether, 4-(benzyloxy) phenol, and methyl tert-butyl ether could form stable benzyl or tert-butyl carbocation by S<sub>N</sub>1 mechanism, and their conversion rates were 0.25,  $7.6 \times 10^{-3}$ , and 6.2, respectively. However, 4-phenoxyphenol, anisole, and cyclohexyl phenyl ether were decomposed via the S<sub>N</sub>2 mechanism. Their conversion rates were  $2.1 \times 10^{-3}$ ,  $1.0 \times 10^{-3}$ , and  $1.1 \times 10^{-3}$ , respectively, which were much slower than those via the S<sub>N</sub>1 mechanism.

For the cleavage of ethers via the S<sub>N</sub>2 mechanism, the structure of the ether influences the conversion rate. First, a strong symmetrical structure, as found in diphenyl ether and dibenzofuran, is less basic and more difficult to be protonated than alkyl ether.<sup>24</sup> Accordingly, their conversion rates were 0. Compared to diphenyl ether, the OH substituent of 4-

**Table 2. Comparison of Hydrothermal Decomposition Rates for Different Ether Compounds**

author	compound	conversion rate (h <sup>-1</sup> )	reaction conditions
Siskin et al. <sup>20</sup>	diphenyl ether	0	250 °C and 5.5 days
	dibenzofuran	0	250 °C and 5.5 days
	4-phenoxyphenol	2.1 × 10 <sup>-3</sup>	250 °C and 5.5 days
	4-(benzyloxy) phenol	7.6 × 10 <sup>-3</sup>	250 °C and 5.5 days
	cyclohexyl phenyl ether	1.1 × 10 <sup>-3</sup>	250 °C and 5.5 days
Katritzky et al. <sup>18</sup>	<i>n</i> -butyl phenyl ether	1.1 × 10 <sup>-4</sup>	250 °C and 3 days
	2,3-dihydrobenzofuran	5.6 × 10 <sup>-4</sup>	250 °C and 3 days
Bagnell et al. <sup>21</sup>	allyl phenyl ether	0.95	230 °C and 1 h
Siskin et al. <sup>19</sup>	1-decyl methyl ether	0	250 °C and 13.5 days
Taylor et al. <sup>22</sup>	methyl <i>tert</i> -butyl ether	6.2	250 °C and 9 min
Wu et al.	anisole <sup>a</sup>	1.0 × 10 <sup>-3</sup>	250 °C and 5.5 days
	benzyl phenyl ether <sup>10</sup>	0.25	250 °C and 4 h
	phenethyl phenyl ether <sup>a</sup>	2.4 × 10 <sup>-3</sup>	250 °C and 5.5 days

<sup>a</sup>Calculated by their corresponding kinetics data from this study.

phenoxyphenol changed its symmetry and offset the electron cloud, which reduced the stability of ether bond. Accordingly, its conversion rate was  $2.1 \times 10^{-3}$ . Second, the ether group also affected the conversion rate. (1) The decomposition of aryl alkyl ether was faster than that of alkyl ether. For example, the conversion rate of anisole was  $1.1 \times 10^{-3}$ , but 1-decyl methyl ether, as an alkyl ether, was not decomposed at all after 13.5 days. (2) For aryl-alkyl ether, the nature of the alkyl group affected the decomposition of the ether bond. For example, phenethyl (phenethyl phenyl ether) and cyclohexyl (cyclohexyl phenyl ether) played a role as alkyls and reduced the electron cloud density of ether bond, and their corresponding phenyl ether conversion rates were  $2.4 \times 10^{-3}$  and  $1.1 \times 10^{-3} \text{ h}^{-1}$ , respectively, which were much faster than those of another alkyl, *n*-butyl ( $1.1 \times 10^{-4} \text{ h}^{-1}$ ).

#### 4. CONCLUSIONS

Investigation of the kinetics of the hydrothermal decomposition of anisole and phenethyl phenyl ether revealed activation energies of  $149.8 \pm 16.4$  and  $143.2 \pm 21.0 \text{ kJ}\cdot\text{mol}^{-1}$  for anisole and phenethyl phenyl ether, respectively. Reaction mechanisms were proposed for both compounds. Cleavage of the lignin ether bond under hydrothermal conditions occurred preferentially at  $\alpha$ -O-4 linkages, with less cleavage at the  $\beta$ -O-4 and methoxy linkages and no cleavage at the stable 4-O-5 linkage. Comparison with the published conversion data of other ethers enabled us to discuss the reactivity of hydrothermal decomposition of ethers.

#### ■ ASSOCIATED CONTENT

##### Supporting Information

Spectral data as mentioned in the text. This material is available free of charge via the Internet at <http://pubs.acs.org>.

#### ■ AUTHOR INFORMATION

##### Corresponding Author

\*Tel./Fax: +86 571 87952683. E-mail address: [jiefu@zju.edu.cn](mailto:jiefu@zju.edu.cn) (J.F.). Tel./Fax: +86 571 87952683. E-mail address: [luxiuyang@zju.edu.cn](mailto:luxiuyang@zju.edu.cn) (X.L.).

##### Notes

The authors declare no competing financial interest.

#### ■ ACKNOWLEDGMENTS

We are grateful to Jun Xiong for assisting with the preparation of PPE. This work was supported by the National High Technology Research and Development Program of China (863 Program, No. 2012AA040211) and the National Natural Science Foundation of China (Nos. 20976160, 21176218).

#### ■ REFERENCES

- (1) Wahyudiono; Sasaki, M.; Goto, M. Recovery of phenolic compounds through the decomposition of lignin in near and supercritical water. *Chem. Eng. Process.* **2008**, *47*, 1609.
- (2) Dorrestijn, E.; Laarhoven, L. J. J.; Arends, I.; Mulder, P. The occurrence and reactivity of phenoxy linkages in lignin and low rank coal. *J. Anal. Appl. Pyrolysis* **2000**, *54*, 153.
- (3) Akiya, N.; Savage, P. E. Roles of water for chemical reactions in high-temperature water. *Chem. Rev.* **2002**, *102*, 2725.
- (4) Fu, J.; Savage, P. E.; Lu, X. Y. Hydrothermal Decarboxylation of Pentafluorobenzoic Acid and Quinolinic Acid. *Ind. Eng. Chem. Res.* **2009**, *48*, 10467.
- (5) Fang, Z.; Sato, T.; Smith, R. L.; Inomata, H.; Arai, K.; Kozinski, J. A. Reaction chemistry and phase behavior of lignin in high-temperature and supercritical water. *Bioresour. Technol.* **2008**, *99*, 3424.
- (6) Bobleter, O. Hydrothermal degradation of polymers derived from plants. *Prog. Polym. Sci.* **1994**, *19*, 797.
- (7) Yokoyama, C.; Nishi, K.; Nakajima, A.; Seino, K. Thermolysis of organosolv lignin in supercritical water and supercritical methanol. *J. Jpn. Pet. Inst.* **1998**, *41*, 243.
- (8) Cheng, L. M.; Ye, X. P.; He, R. H.; Liu, S. Investigation of rapid conversion of switchgrass in subcritical water. *Fuel Process. Technol.* **2009**, *90*, 301.
- (9) Pourali, O.; Asghari, F. S.; Yoshida, H. Production of phenolic compounds from rice bran biomass under subcritical water conditions. *Chem. Eng. J.* **2010**, *160*, 259.
- (10) Wu, X. Y.; Lu, X. Y. Hydrolysis kinetics of benzyl phenyl ether in high temperature liquid water. *Chin. Chem. Lett.* **2011**, *22*, 733.
- (11) Klein, M. T.; Virk, P. S. Model pathways in lignin thermolysis. 1. Phenethyl phenyl ether. *Ind. Eng. Chem. Fundam.* **1983**, *22*, 35.
- (12) Penninger, J. M. L.; Kersten, R. J. A.; Baur, H. C. L. Reactions of diphenylether in supercritical water—Mechanism and kinetics. *J. Supercrit. Fluids* **1999**, *16*, 119.
- (13) Britt, P. F.; Buchanan, A. C.; Malcolm, E. A. Thermolysis of phenethyl phenyl ether—A model for ether linkages in lignin and low-rank coal. *J. Org. Chem.* **1995**, *60*, 6523.
- (14) Crittendon, R. C.; Parsons, E. J. Transformations of cyclohexane derivatives in supercritical water. *Organometallics* **1994**, *13*, 2587.
- (15) Britt, P. F.; Kidder, M. K.; Buchanan, A. C. Oxygen substituent effects in the pyrolysis of phenethyl phenyl ethers. *Energy Fuels* **2007**, *21*, 3102.
- (16) Zipse, H. Radical stability—A theoretical perspective. In *Radicals in Synthesis I: Methods and Mechanisms*; Gansauer, A., Ed.; Springer-Verlag: Berlin, 2006.
- (17) Minami, E.; Kawamoto, H.; Saka, S. Reaction behavior of lignin in supercritical methanol as studied with lignin model compounds. *J. Wood Sci.* **2003**, *49*, 158.
- (18) Katritzky, A. R.; Murugan, R.; Balasubramanian, M.; Siskin, M. Aqueous high-temperature chemistry of carbocycles and heterocycles. 1. Aquathermolysis of acyclic and cyclic phenol ethers in the presence of sodium bisulfite or phosphoric acid. *Energy Fuels* **1990**, *4*, 543.

(19) Siskin, M.; Brons, G.; Katritzky, A. R.; Balasubramanian, M. Aqueous organic-chemistry. 1. Aquathermolysis—Comparison with thermolysis in the reactivity of aliphatic-compounds. *Energy Fuels* **1990**, *4*, 475.

(20) Siskin, M.; Brons, G.; Vaughn, S. N.; Katritzky, A. R.; Balasubramanian, M. Aqueous organic-chemistry. 3. Aquathermolysis—Reactivity of ethers and esters. *Energy Fuels* **1990**, *4*, 488.

(21) Bagnell, L.; Cablewski, T.; Strauss, C. R.; Trainor, R. W. Reactions of allyl phenyl ether in high-temperature water with conventional and microwave heating. *J. Org. Chem.* **1996**, *61*, 7355.

(22) Taylor, J. D.; Steinfeld, J. I.; Tester, J. W. Experimental measurement of the rate of methyl *tert*-butyl ether hydrolysis in sub- and supercritical water. *Ind. Eng. Chem. Res.* **2001**, *40*, 67.

(23) Comisar, C. M.; Hunter, S. E.; Walton, A.; Savage, P. E. Effect of pH on Ether, Ester, and Carbonate Hydrolysis in High-Temperature Water. *Ind. Eng. Chem. Res.* **2008**, *47*, 577.

(24) Streitwieser, A., Jr.; Heathcock, C. H. *Introduction to Organic Chemistry*, 3rd ed.; Macmillan Publishing Co., Inc. and Collier Macmillan Publishers: New York, London, 1985.